Metal–Polymer Nanocomposites Produced by the Melt-Compounding Interaction of an Aliphatic Polyamide with Metal Particles

S. S. Pesetskii,[1] B. Jurkowski,[2] Y. M. Krivoguz,[1] A. A. Davydov,[1] S. P. Bogdanovich[1]

[1]*Laboratory of Chemical Technology of Polymer Composite Materials, V. A. Belyi Metal–Polymer Research Institute, National Academy of Sciences of Belarus, 32a Kirov Street, Gomel 246050, Republic of Belarus*
[2]*Division of Plastic and Rubber Processing, Institute of Material Technology, Poznan University of Technology, 60-965 Poznan, Poland*

Received 11 May 2006; accepted 11 January 2007
DOI 10.1002/app.26240
Published online 23 April 2007 in Wiley InterScience (www.interscience.wiley.com).

ABSTRACT: Composites prepared at 200°C by the melt compounding of copolymer polyamide 6/66 and ferric chloride, ferric oxalate, cupric chloride, cupric formiate, cupric acetate, Cr-carbonyl, Mo-carbonyl, or W-carbonyl have been studied. The solution stability and aggregation suppression for nanoparticles in a polyamide can be explained by the formation of stable polymer–metal complexes. The nitrogen atoms of amide and amine groups of polymers serve as ligands for the coordination compounds that form. The dynamic viscosity of the solutions suggests that Cr-carbonyl forms mostly intermolecular complexes, whereas ferric oxalate, ferric chloride, cupric formiate, cupric acetate, cupric chloride, Cr-carbonyl, Mo-carbonyl, and W-carbonyl form intramolecular complexes. The critical concentrations for metal-containing compounds at which a dispersion rises to nanodimensions without aggregating in the polymer matrix under the experimental conditions are 0.024 wt % for ferric oxalate, 0.12 wt % for ferric chloride, 0.08 wt % for cupric formiate, 0.096 wt % for cupric acetate, and 0.19 wt % for cupric chloride. Metal carbonyls undergo dispersion (with their concentration up to 5 wt %) in polyamide 6/66 without aggregating into larger formations. © 2007 Wiley Periodicals, Inc. J Appl Polym Sci 105: 1366–1376, 2007

Key words: composites; nanotechnology; structure

INTRODUCTION

Nowadays, great interest is being expressed in the production and study of the properties of polymer composites containing inclusions of metals or semiconductors, the dimensions of which are comparable to those of macromolecules.[1–6] The attention to nanodimensional systems (none of the typical linear dimensions of nanoparticles are greater than 100 nm)[6] is caused by the fact that they show unusual physicochemical properties much different from similar properties of substances found in blocklike or microheterogeneous states. In particular, in nanoparticles of metals (in comparison with their larger formations), variations occur in the parameters of the crystal lattice, in atomic dynamics, and in the thermal, electrical, and magnetic properties (an effect of supermagnetism is observed).[6,7] All this makes them promising in the development of nanocomposites to be used as effective and highly selective catalysts,[8] for devices with nonlinear optical features,[9,10] as sensors,[11] and as selective membranes.[12] Metal-containing modifiers are known to be used in the nanodispersed form to improve the mechanical properties of polymeric materials[13,14] and to increase their refractoriness[15] and resistance to thermooxidative aging.[2,16]

The aforementioned effects are dimension-related and strongly depend on the surface conditions of the nanoparticles and interactions between the particles and between the particles and matrix. The properties of individual nanoparticles differ from those of clusters, which form nanosystems.[1,2] Therefore, the methods of producing nanoparticles significantly influence their properties.

There exist a number of methods for synthesizing metal–polymer nanocomposites (1) during the *in situ* formation of inorganic nanoparticles in the course of monomer or oligomer polymerization or within a ready-made polymer matrix;[2,17,18] (2) during the recovery of salts of metals previously introduced into a swollen matrix of blended polymers or copolymers containing certain functional groups;[19] (3) when block copolymers are used, the domains of which can act as microreactors[20,21] (inorganic nanoclusters are formed in one of them); (4) during the thermolysis of decomposable organometallic compounds in a

Correspondence to: S. S. Pesetskii (otdel5mpri@tut.by).
Contract grant sponsor: Belarusian Republic Foundation of Fundamental Investigations; contract grant number: X04P-022.
Contract grant sponsor: Polish State Committee for Scientific Research; contract grant number: 4 TO 8E 067 25.

TABLE I
Physical Properties of MCCs

Compound in the solid state	Color	Temperature (°C)			Solubility in an ethanol/methylene chloride (1 : 1) mixture[a]	Color of the solution
		Melting	Decomposition			
			Onset	Intensive		
Ferric oxalate ($FeC_2O_4 \cdot 2H_2O$)	Yellow		220	260	−	Colorless
Ferric chloride ($FeCl_3$)	Dark red	310	110	215	+	Orange
Cupric formiate [$Cu(HCOO)_2$]	Dark blue		70	215	−	Colorless
Cupric acetate [$Cu(CH_3COO)_2 \cdot H_2O$]	Green	115	140	280	−	Colorless
Cupric chloride [$CuCl_2 \cdot 2H_2O$]	Green	596	95	500	+	Green
Cr-carbonyl [$Cr(CO)_6$]	Colorless	153	90	230	Slightly soluble	Colorless
Mo-carbonyl [$Mo(CO)_6$]	Colorless	148	130	400	Slightly soluble	Colorless
W-carbonyl [$W(CO)_6$]	Colorless	169	148	500	+	Light green

[a] + = easily soluble; − = insoluble.

polymer environment under the effects of temperature and ultrasound;[6,22] (5) when a solution of a polymer and a metal-containing compound (MCC) is being prepared with subsequent evaporation of the solvent;[23] and (6) when metal nanoparticles are produced in natural pores of polymeric matrices (e.g., polyolefins and polytetrafluoroethylene) with a high rate of the thermal decomposition of monomolecules in solutions of metal compounds in a molten polymer.[24–26] In such cases, the uniform size and shape distribution of the solid particles are stabilized by interactions with the polymer matrix. Researchers have much less investigated the opportunities for the elaboration of metal–polymer nanocomposites based on technologies closely approaching modern, highly efficient processes intended for the melt compounding of thermoplastic polymers (e.g., to make polymer–clay nanocomposites).[27–29] Therefore, it is important to understand the rules of metal-nanoparticle generation in a polymer matrix when nanocomposites are prepared by an extrusion technique.

In most available studies devoted to the production of such composites, the polymer matrices have been polyolefins and polytetrafluoroethylene,[2,24–26,30] which show a low reactivity toward metals and ions of metals because of their low polarity and the absence of chemically active functional groups in their macromolecules. One might expect that polar polymers, containing reactive groups when in contact with metal nanoparticles, would interact, thus leading to the formation of unusual structures and imparting novel properties to the materials. Among such polymers are aliphatic homopolymers and copolymers.[31]

The chemical structure of polyamide 6/66 (PA6/66), a commercially manufactured copolymer, consists of fragments of polyamide 6 and polyamide 66 macromolecules. Because of this, it can be assumed that the character of the interactions with MCCs will be similar to that of the aforementioned homopolymers.

The aim of this work was to investigate nanocomposites produced by the melt compounding of a PA6/66 aliphatic copolymer with MCCs, which include the complex-forming ions of transition metals. Of particular interest was the determination of the interaction specificity of the polymers with metal nanoparticles with respect to the nature of the MCC used.

EXPERIMENTAL

Materials

The initial PA6/66 copolymer was produced by the copolymerization of ε-caprolactam (50%) and adipic hexamethylene diamine (50%), as supplied by Ural Plastics (Ekaterinburg, Russia; density = 1.11 g/cm^3, melting point = 169°C, crystallization temperature = 125°C). PA6/66 was easily dissolved in a mixture of ethanol and methylene chloride with a weight ratio of 1 : 1. Salt compounds of iron and copper and carbonyls of transition metals were used to prepare nanocomposites. Some of the properties of these compounds are given in Table I. The characteristic temperatures were determined by differential thermal analysis (DTA) at a heating rate of 6.25°C/min. The compounds were chosen so that they would contain transition metals, thus being efficient complex-forming agents. The substances themselves were supposed to be soluble in molten PA6/66, melt at a temperature below the compounding temperature, or decompose at that temperature and give off all chemically active metal particles, metal oxides, or some other products of thermal transformations.

Production of the metal-containing nanocomposites

The nanocomposites were produced by the melt compounding of PA6/66 with a single-screw extruder (screw diameter = 36 mm, length/diameter = 17) equipped with a static mixer.[32] The shear rate

of the melt moving through the mixer discs was about 100 s^{-1}. Before the compounding, PA6/66 had been dried *in vacuo* at 90°C for 6 h to escape any influence of the residual moisture on the hydrolytic degradation of the macromolecules during compounding. Before being loaded into the extruder, the MCCs were mixed with PA6/66 granules in a twin-blade turbo mixer. The concentrations of the additives (MCCs) ranged from some hundredths of a percent up to 5 wt %. The compounding temperature in the static mixer and in the output zone of the extruder was constant: 200°C. The residence time for the melt at this temperature was about 4 min in all cases. The product, in the form of strands of 3–4 mm in diameter, were water-cooled and granulated. The dried granules were injection-molded to produce the test specimens in the form of 80 mm × 10 mm × 4 mm plates. Those were intended to study the material's structure as well as the particle distribution within the polymer and also to make tensile test pieces in the form of dog bones, the neck of which measured 45 mm × 5 mm × 3 mm.

Thermal analysis

The MCC specimens were subjected to DTA (Q-1500 derivatograph, Optics Plant, Budapest, Hungary; heating rate = 6.25°C/min). Thermograms were taken in air.

IR spectroscopy

A Nexus (Atkinson, NH) 5770 IR spectrophotometer with Fourier transformation was employed. Absorption spectra were taken from films 20–30 μm thick and compression-molded at 190°C.

Estimation of the light transmission

The optical transparency of solutions of the composites was estimated with an FM-58 (JSC ''ZOMZ,'' Zagorsk, Russia) visual photoelectric photometer. Glass cells and a light filter with $\lambda = 597$ nm were adopted.

X-ray analysis

The study was made by wide-angle X-ray analysis with a DRON-3 (SIU ''Burevestnik,'' Leningrad, Russia) diffractometer, Cu Kα radiation, a nickel filter, and a reflection procedure. The rotation rate of the X-ray quantum counter was 2°/min; that of specimen was 1°/min. The presence of aggregates of the metal-containing phase in the composite was estimated from reflexes typical for that phase in diffraction patterns of PA6/66.

Rheological study

The dynamic viscosity of the polymer and composites was determined with a Rheotest-2 rotary viscosimeter (HAAK Mess-Technik Gmbh U. Co., Karlsruhe, Germany). The coaxial cylinder measuring system was used. For the analysis, a solution temperature of 25°C was taken. The shear rates were between 0.02 and 1.3 × 10^3 s^{-1}.

Scanning electron microscopy (SEM) with chemical microanalysis

This technique was adopted to estimate the distribution and dispersivity of metals and MCCs in PA6/66. The analysis was performed on a JSM (Jeol Ltd., Tokyo, Japan) 5610 LV microscope with an EDXJED 2201 energy-dispersion chemical analysis device equipped with ZAF (atomic number, absorption, and fluorescence) correction and the Phi-Rho-Z method. The microscope resolution was 3 nm. The latter allowed the calculation of the content of light chemical elements in the specimen. SEM pictures of the surface and distribution maps of the elements were taken under a low vacuum at a residual gas pressure of 20 Pa and an accelerating voltage of 30 kV. These specimens were in the form of plates, as described in a previous section. After cooling in liquid nitrogen for 30 min, the plates were subjected to brittle fracture. The chipped surfaces were examined.

RESULTS AND DISCUSSION

Interaction of molten PA6/66 with metals and MCCs

The analysis of the composites shows that they possess typical qualities of metal-complex compounds. Solutions of all the composites are colored (Table II). This is one of the signs of their complex formation.[33] Typically, compounds that are insoluble in their original state become soluble in an ethanol/methylene chloride mixture when incorporated into PA6/66 (Tables I and II).

Taking into consideration the fact that PA6/66 forms colorless solutions in an ethanol/methylene chloride mixture, we can conclude that the interaction of soluble metal compounds (metal carbonyls and cupric chloride) with polyamide (PA) leads to the color change of the solutions.

The introduction of MCCs into PA6/66 causes noticeable changes in its IR spectrum (Fig. 1). The addition of ferric chlorides and cupric chlorides changes the shape of the band at 1280 cm^{-1} [amide IV; Fig. 1(2)]. There appear kinks in the νNH vibration bands [3075 and 3300 cm^{-1}; Fig. 1(3)].

No changes have been detected in the area of the fundamental vibrations of PA bands: amide I (1660 cm^{-1})

TABLE II
Characteristics of Solutions of PA6/66 Composites with 3 wt % Concentrations of MCCs

MCC	Ferric oxalate	Ferric chloride	Cupric formiate	Cupric acetate	Cupric chloride	Cr-carbonyl	Mo-carbonyl	W-carbonyl
Color of solution	Orange	Dark orange	Dark green	Bright green	Light green	Green	Yellow	Yellow
Transmission coefficient of the solution (%)[a]	26.2	24	18.6	21.0	24.7	26.8	27.6	28.1
Presence of metal in the precipitate	Present	Absent	Present	Present	Absent	Absent	Absent	Absent

[a] The concentration of the solution was 5 wt %.

and amide II (1560 cm^{-1}). Typical for all the MCCs is the shifting of the νNH band into the high-frequency region. The shift magnitude depends on the nature of the modifier (Fig. 2 and Table III). The largest shifts have been observed for Cr-carbonyl (20 cm^{-1}), cupric chlorides, ferric chlorides, and W-carbonyl (15 cm^{-1}).

The results of the IR spectroscopy analysis bear witness for the presumption that PA6/66 macromolecules form complexes with metals and MCCs. As no qualitative changes are observed in the band of amide I (ν > C = 0), it can be assumed that a coordination interaction occurs through nitrogen atoms of amide groups.

Nitrogen atoms with their free electron pair are reactive ligands with σ-donor qualities.[33,34] Bands related to the valence vibrations of the metal–ligand have been found between 100 and 800 cm^{-1};[33] they are weak and not typical of different bonds. Therefore, most information on the structure of the complexes is obtained from the location analysis of the bands typical of ligands. Changes in the electron density in a ligand under the action of the central atom result in variations of its bond number. This shifts the characteristic bands into the long-wave or short-wave region. Long-wave shifts occur most often. An increase in the bond number can cause an increase in the frequency. High-frequency shifts have been observed for symmetrical vibrations of C=O groups, belonging to carboxyl groups of protein amino acids, during their complex formation with metals.[35]

Increases of 15–32 cm^{-1} in the frequency of valence vibrations have also been observed for the N=C band in azomethines coordinated with ferric chloride.[36] Such increases are also characteristic of numerous carboxyl complexes.[37]

In our case, the short-wave shift of the νNH band can be explained by the fact that the formation of a metal–nitrogen atom complex causes an additional shift of the electron density from hydrogen atoms toward nitrogen, and the NH bond becomes stronger.

A fine dispersion of MCC in PA6/66 along with complex formation must change the intensity of the molecular interactions between macromolecules. The dynamic viscosity of polymer solutions and melts is a parameter rather sensitive to variations in the poly-

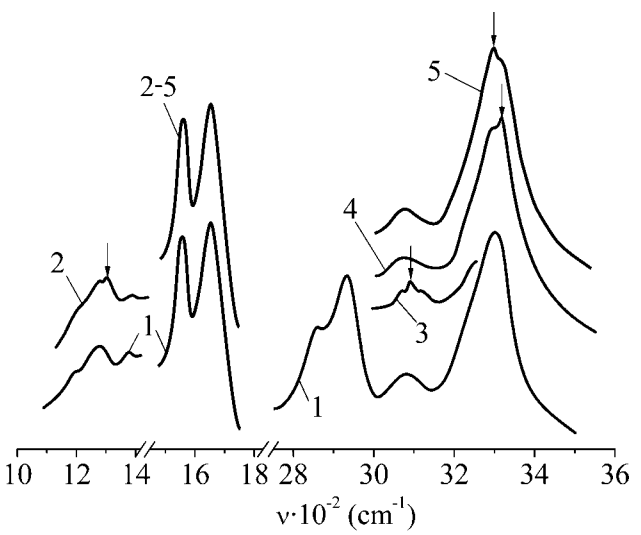

Figure 1 Characteristic changes in the IR spectrum of PA6/66 after MCC was added: (1) PA6/66; (2) PA6/66 modified with ferric chloride and cupric chloride; (3) PA6/66 modified with Cr-carbonyl, cupric acetate, and cupric chloride; (4) PA6/66 modified with Cr-carbonyl and ferric chloride; and (5) PA6/66 modified with W-carbonyl and Mo-carbonyl.

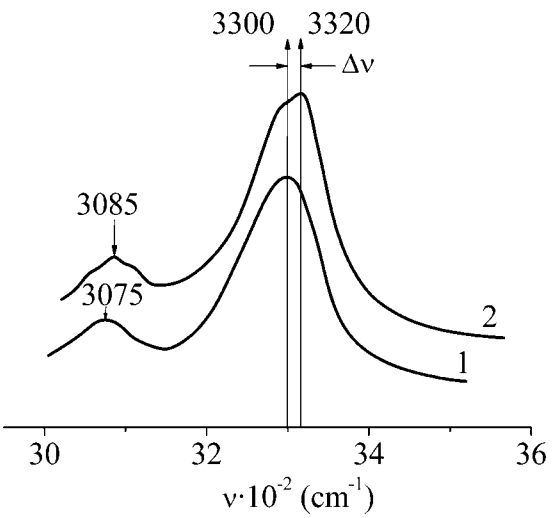

Figure 2 Absorption bands of νNH in the IR spectra of (1) PA6/66 and (2) PA6/66 containing Cr-carbonyl (3 wt %).

TABLE III
Effect of MCCs on the Location of the *ν*NH band in the IR Spectra of PA6/66

MCC[a]	νNH (cm^{-1})	ΔνNH (cm^{-1})
PA6/66	3300	
Ferric oxalate	3305	+5
Ferric chloride	3315	+15
Cupric formiate	3305	+5
Cupric acetate	3312	+12
Cupric chloride	3315	+15
Cr-carbonyl	3320	+20
Mo-carbonyl	3310	+10
W-carbonyl	3315	+15

[a] The concentration of the MCC was 3 wt %.

mer chemical structure.[38] Therefore, we have used the rheological procedure to analyze the types of coordination bonds formed. Figure 3 shows that the viscosity of a composite solution is usually lower than that of the initial PA6/66 (curve 1 stands for the flow of the PA6/66 solution and is given in all the plots to make the comparison of the results more illustrative). The viscosity rise is a result of intensified intermolecular interactions in PA6/66, which in this case might be caused only by intermolecular complex formation. It can be assumed, therefore, that Cr-carbonyl added to PA6/66 leads to intermolecular complex formation. The other modifiers form mostly intramolecular complexes with polymers. Obviously, the lower the dynamic viscosity is, which is caused by high shear rates (in comparison with that of the unmodified PA6/66 solution), the stronger the metal–ligand coordination bond is. If the viscosity is similar or close to that of the initial PA6/66, then it can be assumed that the coordination bond that forms is weak and fails by shearing. As a result, the character of the intermolecular interactions in a modified PA will resemble that of the initial polymer, and this implies that their viscosity is of a similar value. In view of this, it follows that the strongest intramolecular complexes are formed with ferric chlorides [Fig. 3(a-2)], cupric chloride [Fig. 3(b-2)], and Mo-carbonyl [Fig. 4(c-3)].

The concentration/dynamic viscosity relationships have proved the fact of intermolecular complex formation in the case of Cr-carbonyl [Fig. 4(d)]. With increasing Cr-carbonyl concentration, the viscosity grows over a wide range of shear rates. In our opinion, high concentrations of ferric oxalate change the manner of the complex formation [Fig. 4(c-1)]. The complexes that form, however, are weak because they break down when the shear rate is raised [Fig. 4(c-2,c-3)].

The differences in the rheological behavior of the materials are not associated with PA degradation during compounding. This conclusion is supported by a lack of a direct correlation between the degradation temperature of the composites (Table IV) and their solution viscosity (Figs. 3 and 4). Besides, the mechanical properties of the materials differed only negligibly from those of the initial PA6/66 (Table IV).

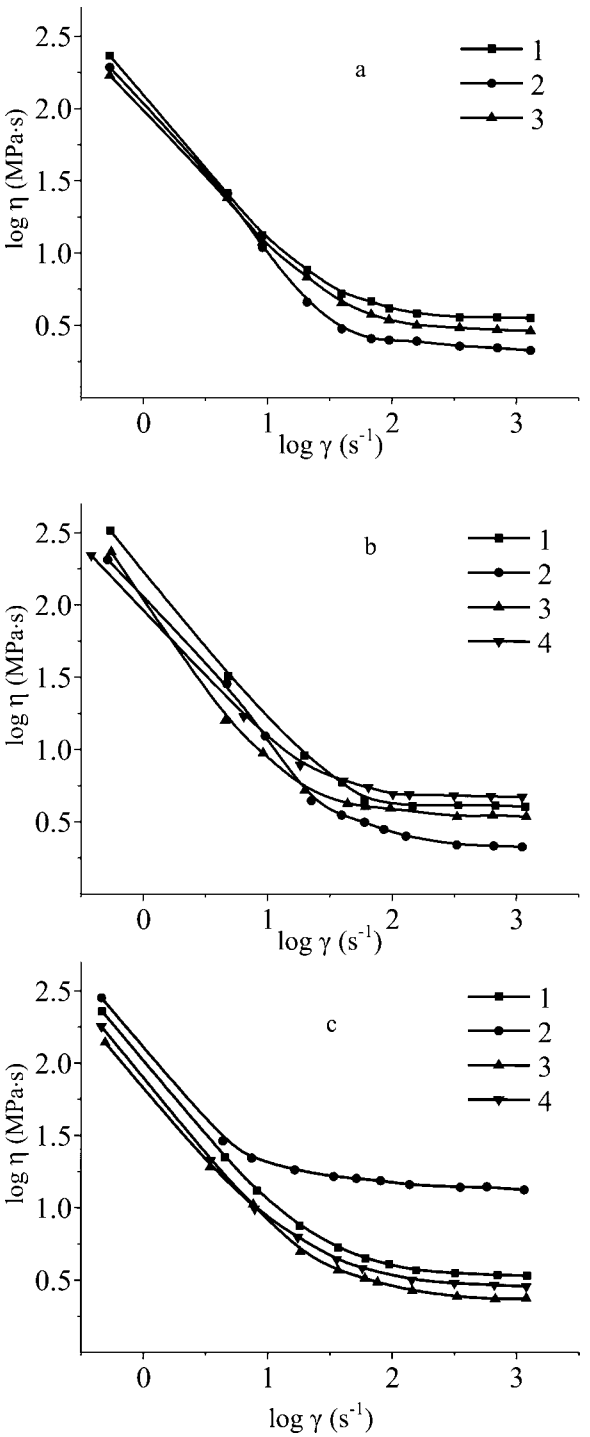

Figure 3 Logarithm of the dynamic viscosity (η) versus the logarithm of the shear rate (γ) for (1) PA6/66 solutions and (2–4) solutions of PA6/66 modified with MCCs (3 wt %): (a-2) ferric chloride, (a-3) ferric oxalate, (b-2) cupric chloride, (b-3) cupric acetate, (b-4) cupric formiate, (c-2) Cr-carbonyl, (c-3) Mo-carbonyl, and (c-4) W-carbonyl. The solution concentration was 5 wt %.

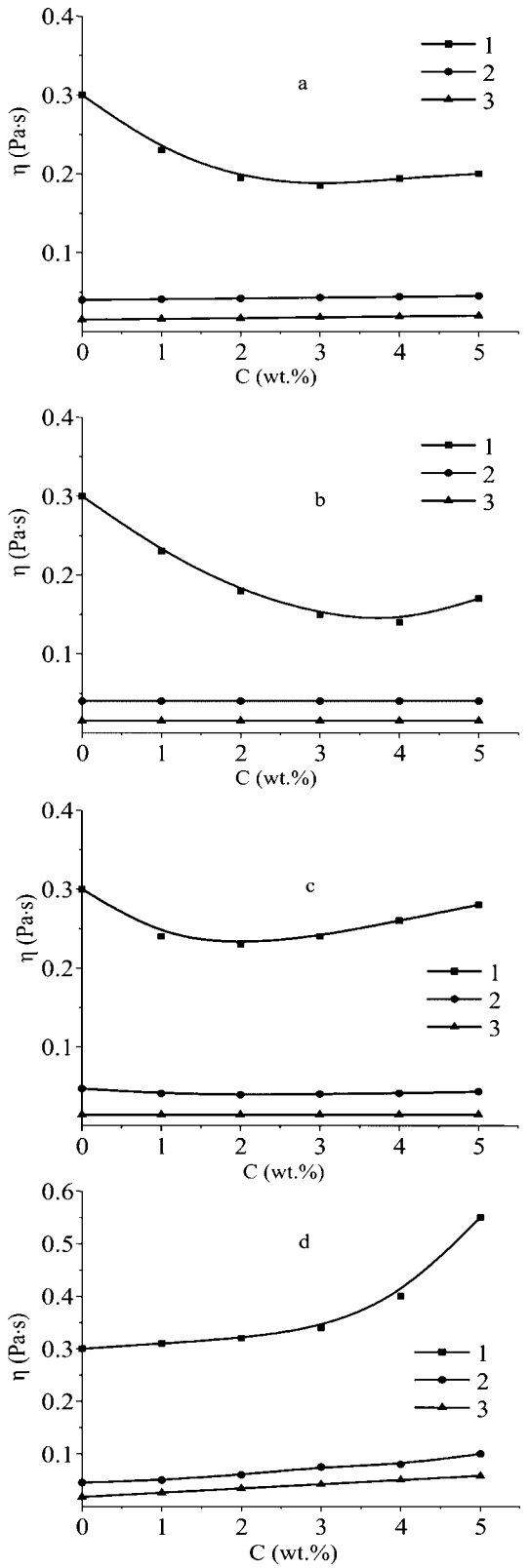

Figure 4 Concentration (C) of MCC in PA6/66 composites against the dynamic viscosity (η) of their solutions: (a) cupric formiate, (b) Mo-carbonyl, (c) ferric oxalate, and (d) Cr-carbonyl. The shear rate was (1) 0.5, (2) 4, or (3) 730 s^{-1}. The solution concentration was 5 wt %.

Distribution of MCCs in PA6/66

Nanocomposite solutions

Solutions of microheterogeneous metal–polymer systems are sedimentarily unstable.[39] Because of this, in addition to fine dispersions of metal-containing modifiers and their coordination bonding, the aggregation of particles is quite possible, leading to independent microphases. Aggregation in such systems can be investigated in view of the variations in the optical density of the solutions.[40]

Plots of the concentration versus the transmission coefficient for solutions of composites containing ferric oxalate, cupric formiate, and cupric acetate show kinks when the modifier concentration is between 0.05 and 0.3 wt % [Fig. 5(a)]. The kinks are explained by the aggregation onset for particles of the metal-containing phase. As aggregation occurs in addition to coordination, the transmission coefficient varies to a smaller extent with increasing concentration than it does before the moment of aggregation onset (particle aggregation weakens the depth intensity of coloring because of the growing concentration of complexes). A photometry estimation of aggregation in solutions of composites containing metal carbonyls and metal chlorides is impossible because these solutions do not produce precipitates of the aggregated phase [Fig. 5(b)].

Solid-phase systems

To estimate the aggregation of metals and their compounds in the polymer in the solid phase, radiography[41] or, naturally, electron microscopy can be used. A comparison of diffraction patterns for MCCs in Figure 6 with those for PA6/66 in Figure 7 shows that each of the tested compounds gives reflexes that do not overlap the peak in the radiogram of partly crystallized PA. Consequently, the spectra for modifiers can easily be recorded over the PA6/66 spectrum.

For some of the composites, X-ray spectra are given in Figure 7(2–7). Here, the PA6/66 diffraction patterns do not show the spectra of metal carbonyls only. A more detailed analysis of how the metal carbonyl concentrations influence the character of the spectra obtained with Mo-carbonyl reveals that the carbonyl phase cannot be recorded by radiography techniques if its concentration in PA is below 5 wt % (Fig. 8).

By extrapolating the concentration dependence of the reflex intensities of characteristic peaks (for ferric oxalate, the reflex has a maximum at $2\theta = 18^\circ 40'$; for ferric chloride, $2\theta = 15^\circ 20'$; for cupric formiate, $2\theta = 44^\circ 10'$; for cupric acetate, $2\theta = 13^\circ$; for cupric chloride, $2\theta = 16^\circ 30'$) up to the intersection with the abscissa, we can determine a minimal

TABLE IV
Temperature of 20 wt % Loss ($T_{20\%}$), Yield Point in Elongation (σ), and Relative Elongation at Rupture (ε) During the Dynamic Heating of MCCs Based on PA6/66

	Fe		Cu			Carbonyl			
MCC	Oxalate	Chloride	Formiate	Acetate	Chloride	Cr	Mo	W	PA6/66
$T_{20\%}$ (°C)	390	394	417	415	392	417	418	410	416
σ (MPa)	24	22	24	27	23	28	26	28	23
ε (%)	390	468	422	359	303	417	385	425	414

The heating rate was 6.25°C/min. The concentration of the MCC was 3 wt %.

concentration of an MCC that does not undergo aggregation in the polymer phase (Fig. 9). One can see that the concentration of the MCC associated with the complexes without aggregates is low, and depending on the nature of the modifier, it can be tenths or even hundredths of a weight percent (Table V).

The suitability of this approach for estimating the aggregation of MCCs in PA is known.[41] It has been reported that the basic reflexes of MCCs in PA are rather tentative.

As for the metal carbonyls, their increased solubility in the molten PA is obvious in comparison with other compounds. It is possible, however, that the

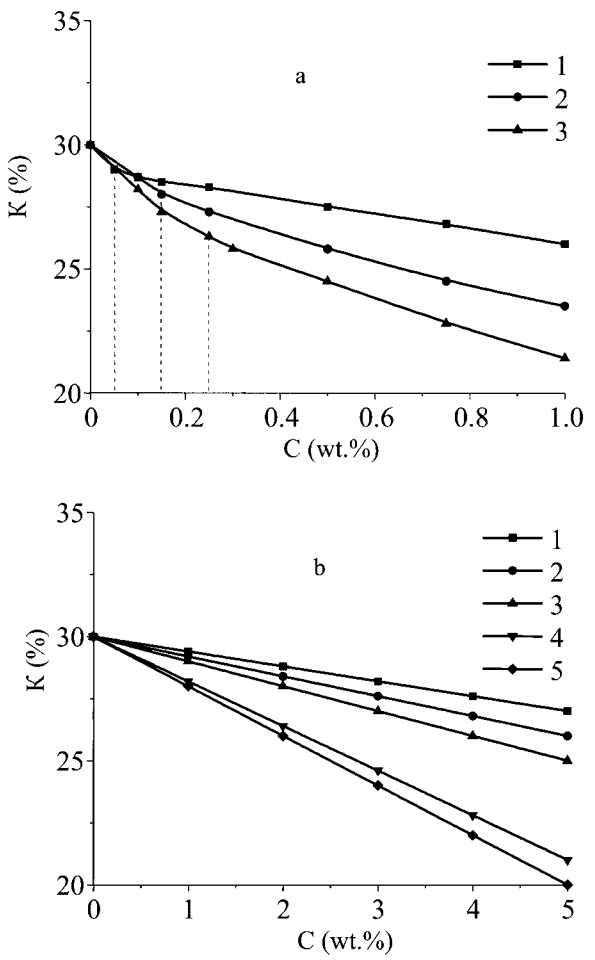

Figure 5 Transmission coefficient (K) for PA6/66 solutions containing 3 wt % of the following: (a-1) ferric oxalate, (a-2) cupric acetate, (a-3) cupric formiate, (b-1) Mo-carbonyl, (b-2) W-carbonyl, (b-3) Cr-carbonyl, (b-4) cupric chloride, and (b-5) ferric chloride.

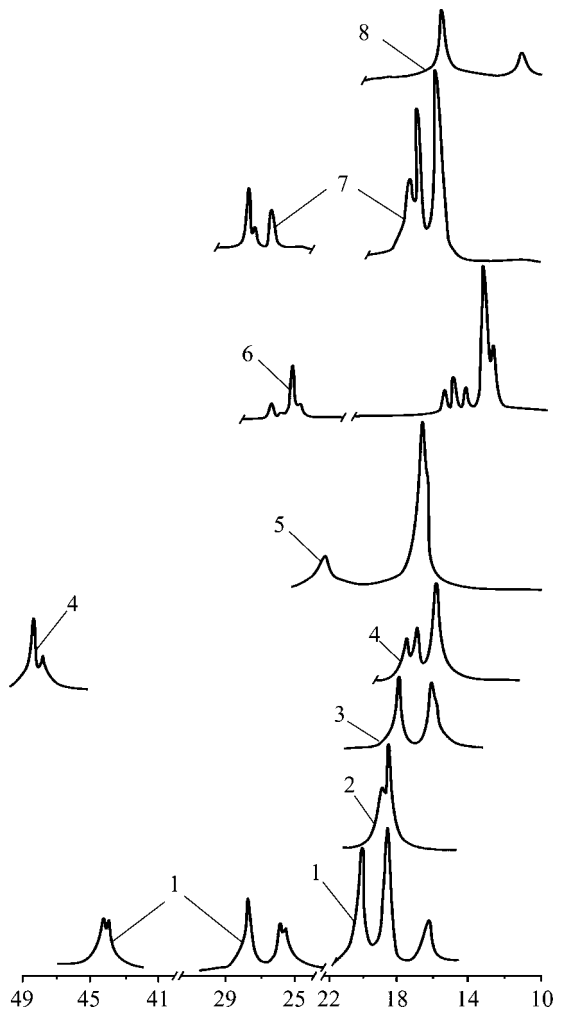

Figure 6 Wide-angle diffraction patterns for (1) cupric formiate, (2) ferric oxalate, (3) Cr-carbonyl, (4) Mo-carbonyl, (5) cupric chloride, (6) cupric acetate, (7) Mo-carbonyl, and (8) ferric chloride.

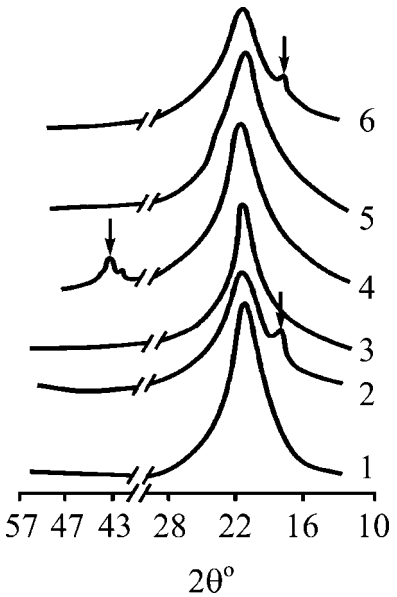

Figure 7 Wide-angle diffraction patterns for (1) PA6/66 and (2–5) its composites with 3 wt % of the following: (2) ferric oxalate, (3) Mo-carbonyl, (4) cupric formiate, (5) Cr-carbonyl, and (6) cupric chloride.

aggregates undetectable by radiography can be of two types: either carbonyl aggregates or aggregates containing products of the thermal dissociation of carbonyl groups.

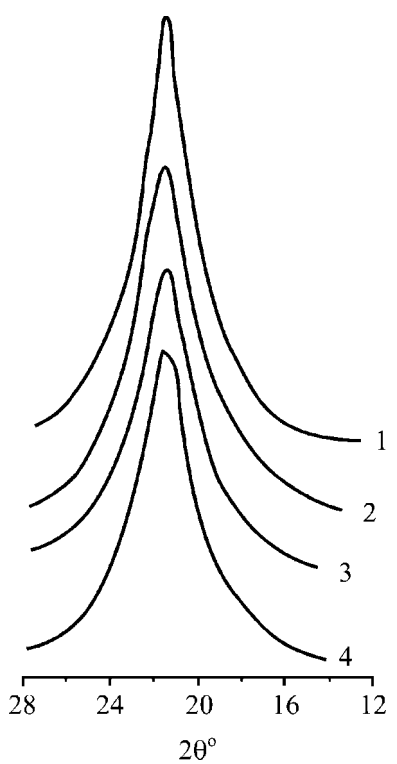

Figure 8 Wide-angle diffraction patterns for PA6/66 composites containing Mo-carbonyl: (1) 0.2, (2) 1.0, (3) 3.0, and (4) 5.0 wt %.

The tested MCCs can completely or partly decompose in the PA6/66 phase when composites are being prepared. The resulting products of decomposition are chemically active metals or their oxides or chlorides.[16,23,42,43] The reactions of thermal decomposition can be schematically represented as follows:[16,23]

- Ferric oxalate: $FeC_2O_4 \cdot 2H_2O \rightarrow Fe + 2CO + 5CO_2 + 6H_2O + Fe_2O_3$
- Ferric chloride: $2FeCl_3 \rightarrow 2FeCl_2 + Cl_2$
- Cupric formiate: $Cu(HCOO)_2 \rightarrow Cu + 2CO_2 + H_2$ and $Cu(HCOO)_2 \rightarrow CuO + CO + CO_2 + H_2$
- Cupric acetate: $Cu(CH_3COO)_2 \cdot H_2O \rightarrow Cu + 2C + 2CO_2 + H_2O + 6H_2$
- Cupric chloride: $CuCl_2 \cdot 2H_2O \rightarrow CuCl_2 + 2H_2O$ and $2CuCl_2 \rightarrow 2CuCl + Cl_2$
- Metal carbonyls: $M(CO)_n \rightarrow M + nCO$

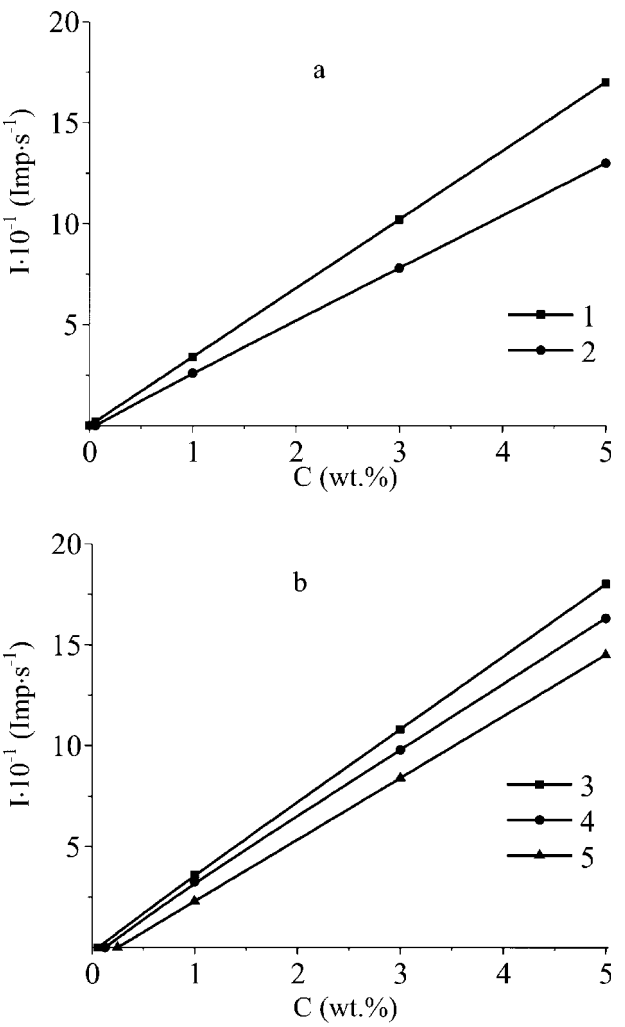

Figure 9 Concentration (*C*) of MCC and intensity (*I*) of the peaks (in the reflexes typical for them) in diffraction patterns of PA6/66 composites containing (1) ferric oxalate, (2) ferric chloride, (3) cupric formiate, (4) cupric acetate, and (5) cupric chloride.

TABLE V
Concentrations of the MCCs Dispersed in PA6/66 up to Nanoparticles Without Agglomeration

	Fe		Cu			Carbonyl		
MCC	Oxalate	Chloride	Formiate	Acetate	Chloride	Cr	Mo	W
Concentration of the compound (wt %)	0.05	0.2	0.2	0.3	0.5	>5	>5	>5
Concentration on a pure metal basis (wt %)	0.024	0.12	0.08	0.096	0.19			

It is possible, therefore, for the initial modifiers, or products of their thermal dissociation, to participate in forming complexes with PA6/66 macromolecules. As a result, the composition of the metal–polymer complexes that form is rather complicated. It is quite probable that metals with neutral electrons, as well as their ions, take part in complex formation. Their formation may lead to the ionization of metals.[3,5] In the case of metal carbonyls, mixed ligand complexes may be formed that include, as ligands, CO and amino groups of macromolecules.[44]

To estimate visually the distribution of MCC in PA6/66, analyses were performed of chip surfaces obtained from injection-molded specimens (80 mm $\times$ 10 mm $\times$ 4 mm). A specimen was first exposed to liquid nitrogen for 30 min. Then, it was fastened in a clamp, and chips were cut with a sharp steel knife. For the electron microscopy examination, the chip surface was taken from the middle zone of the specimen. To obtain more detailed information about the distribution character of the MCCs in the polymer, SEM photomicrographs of the test surfaces and dis-

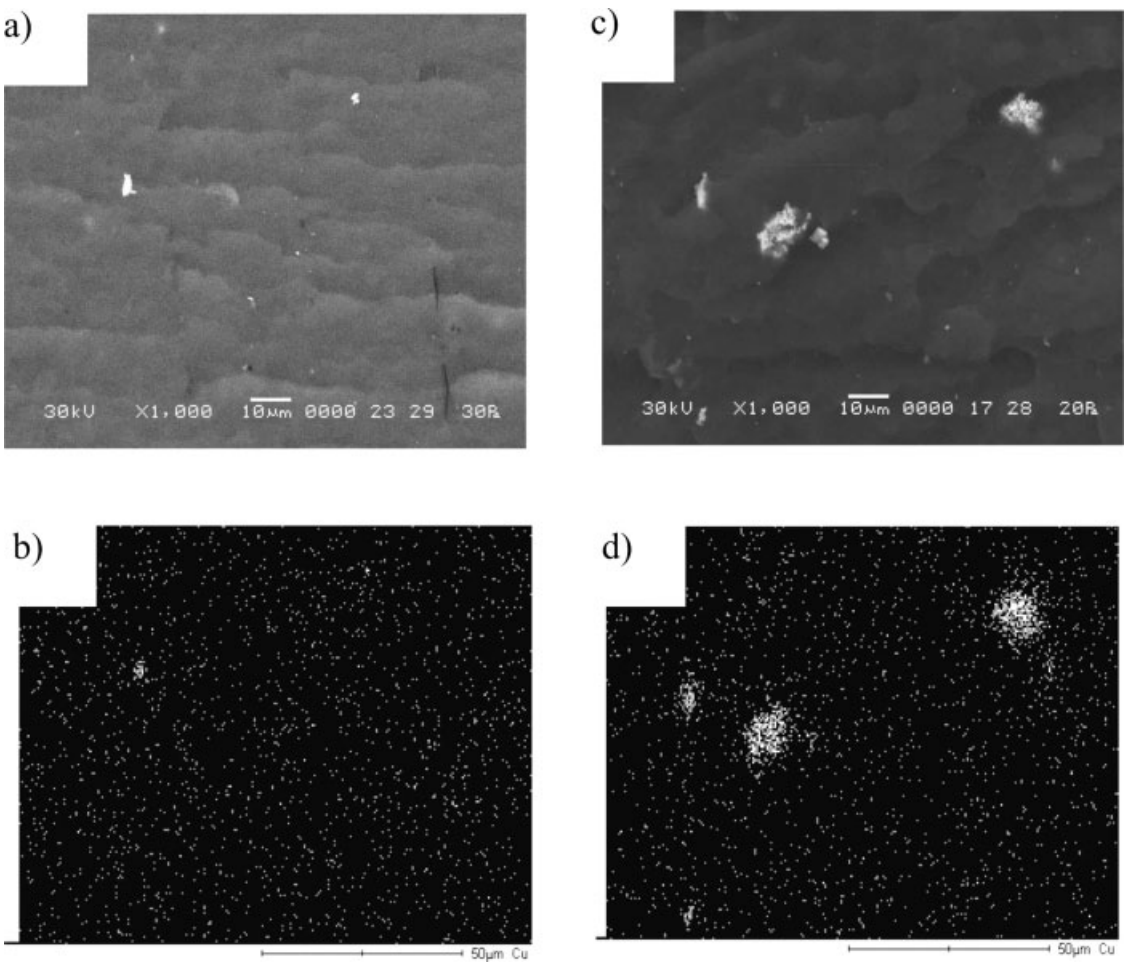

Figure 10 (a,c) SEM photomicrographs and (b,d) distribution maps of copper in the polymer for PA6/66 composites containing cupric formiate: (a,b) 0.2 and (c,d) 3.0 wt %.

tribution maps of the metal atoms in the polymer were taken.

The results of electron microscopy appear to correlate with the data obtained by wide-angle X-ray scattering. For example, at an MCC concentration equal to or below that at which particles aggregate in the polymer (Table V), the dimensions of the metal inclusions do not exceed 10 nm. At higher concentrations, aggregates reach sizes of micrometers. This can be concluded particularly from Figure 10, in which the results are given for composites of PA6/66 with cupric formiate. With 3 wt % cupric formiate, the aggregates could be as large as 5 μm. It should be noted that a similar picture is typical of composites of PA6/66 with all the MCCs tested; the exception is metal carbonyls. The size of the nanoparticles that formed in the latter composites did not exceed 5 μm for any of the concentrations tested. This may be explained by the high solubility of the carbonyls in the molten PA. Besides, it is quite possible that gaseous products released during the thermal decomposition of carbonyls in the PA6/66 environment cause additional turbulization in the molten polymer, thus increasing the degree of homogenization of the material as well as the dispersity of the nanoparticles. It should be noted that a high dispersivity of metal-containing particles up to 1–5 nm is typical of metal carbonyl thermolysis in other polymers, such as ultradispersed polytetrafluoroethylene.[30]

CONCLUSIONS

Metal–polymer nanocomposites can be obtained by the melt compounding of PA6/66 with MCCs (e.g., ferric chloride, ferric oxalate, cupric chloride, cupric formiate, cupric acetate, and carbonyls of Cr, Mo, and W) with an extruder equipped with a static mixer. Transition metals form coordination bonds with PA. Nitrogen atoms of amide groups act as ligands of formed coordination bonds. The metal–polymer compounds are soluble in an ethanol/methylene chloride (1 : 1) mixture and give solutions of different colors. The solution stability (no precipitates of MCC have been detected) and absence of nanoparticle aggregates (no metal clusters have been formed) in the solid polymer matrix can be explained by the formation of stable metal–polymer complexes.

The limiting concentrations (calculated on a pure metal basis) of MCCs, up to which the dispersion process causes no nanoparticle aggregation in the polymer under the experimental conditions, are 0.024 wt % for ferric oxalate, 0.12 wt % for ferric chloride, 0.08 wt % for cupric formiate, 0.096 wt % for cupric acetate, and 0.19 wt % for cupric chloride. Metal carbonyls (with their concentration up to 5 wt %) disperse in PA6/66 into nanoparticles up to 1–5 nm without forming any aggregates of larger dimensions.

References

1. Chvalun, S. N. Russ J Prir 2000, 7, 53.
2. Pomogailo, A. D.; Rozenberg, A. S.; Urliand, I. E. Metal Nanoparticles in Polymers (in Russian); Khimia: Moscow, 2000.
3. Roldugin, V. I. Usp Khim 2000, 69, 899.
4. Mansur, H. S.; Vasconcelos, W. L.; Grieser, F.; Caruso, F. J Mater Sci 1999, 34, 5285.
5. Hao, E.; Lian, T. Langmuir 2000 16, 78.
6. Gubin, S. P.; Koksharov, Y. A.; Khomutov, G. B.; Yurkov, G. Y. Russ Chem Rev 2005, 74, 539.
7. Barthelemy, A.; Fert, A.; Morel, R.; Storen, L. Phys World 1994, 7, 34.
8. Chu, J. W.; Shim, J. W. J Mol Catal 1993, 78, 189.
9. Olsen, A. W.; Kafafi, Z. H. J Am Chem Soc 1991, 113, 7758.
10. Vossmeyer, T.; Katsikas, L.; Giersig, M.; Popovic, I. J Phys Chem 1994, 98, 7665.
11. Hopf, H.; Gerasimov, G. N.; Chvalun, S. N.; Rozenberg, V. J.; Popova, E. L.; Nikolaeva, E. V.; Grigorjev, E. I.; Savjalov, S. A.; Trakhtenberg, L. I. Adv Mater Chem Vap Deposition 1997, 3, 197.
12. Rigbi, Z. Adv Polym Sci 1980, 36, 21.
13. Grishin, B. S.; Pisarenko, T. I.; Evstratov, V. F. Dokl Akad Nauk 1991, 321, 321.
14. Breval, E.; Mulvihill, M. L.; Dongherry, J. P.; Vemuham, R. E. J Mater Sci 1992, 27, 3297.
15. Subbulakshmi, M. S.; Kasturiya, N.; Hansra, J.; Bajai, P.; Agarwal, R. Rev Macromol Chem Phys 2000, 4, 85.
16. Gladyshev, G. P.; Ershov, Y. A.; Shystova, O. A. Stabilization of Heat Resistant Polymers (in Russian); Khimia: Moscow, 1979.
17. Khairutdinov, R. F. Usp Khim 1998, 67, 125.
18. Gerasimov, G. N.; Bochilin, V. A.; Chavlun, S. N.; Volkova, L. V.; Kardash, I. Y. Macromol Chem Phys 1996, 197, 1387.
19. Volkov, A. V.; Karachevtsev, I. V.; Moscvina, M. A.; Rebrov, A. V.; Volynskii, A. L.; Bakeev, N. F. J Inorg Organomet Polym 1995, 5, 295.
20. Brown, R. A.; Masters, A. J.; Coloin, P.; Yung, X. F. Compr Polym Sci 1989, 2, 6.
21. Möller, M.; Zentz, D. W. Macromol Chem 1989, 190, 1153.
22. Syrkin, V. G. Carbonyls of Metals (in Russian); Khimia: Moscow, 1983.
23. Natanson, E. M.; Ulberg, Z. R. Colloid Metals and Metallopolymers (in Russian); Naukova Dumka: Kiev, 1971.
24. Gubin, S. P.; Kosobudskii, I. D.; Petrakovskii, G. I.; Piskorskii, V. P.; Kaskina, L. V.; Kolomeichuk, V. N. Dokl Akad Nauk 1981, 260, 655.
25. Gubin, S. P.; Kosobudskii, I. D. Dokl Akad Nauk 1983, 272, 1155.
26. Gubin, S. P. Colloids Surf A 2002, 202, 155.
27. Fornes, T. D.; Yoon, P. J.; Keskkula, H.; Paul, D. R. Polymer 2001, 42, 9929.
28. Cho, J. W.; Paul, D. R. Polymer 2001, 42, 1083.
29. Hagesawa, N.; Okanoto, H.; Kawasumi, M.; Kato, M.; Tsukigase, A.; Usuki, A. Macromol Mater Eng 2000, 280, 76.
30. Buznik, V. M.; Fomin, V. M.; Alhimov, A. P.; Ignateva, L. I.; Tsvetkov, A. K.; Kudryavyi, V. G.; Kosarev, V. F.; Gubin, S. P.; Lomovskii, O. I.; Okhlopkova, A. A.; Uvarov, N. F.; Klinkov, S. V.; Shabalin, I. I. Metal–Polymer Nanocomposites (in Russian); Siberian Branch of the Russian Academy of Sciences: Novosibirsk, 2005.
31. Nylon Plastics Handbook; Kohan, M. I., Ed.; Hanser: Munich, 1995.

32. Pesetskii, S. S.; Jurkowski, B.; Krivoguz, Y. M.; Urbanowicz, R. J Appl Polym Sci 1997, 65, 1493.
33. Skorik, N. A.; Kumok, V. I. Chemistry of Coordination Compounds (in Russian); Vysshaya Shkola: Moscow, 1975.
34. Kukushkin, Y. N. Ligands for Coordination Compounds (in Russian); Leningrad University: Leningrad, 1981.
35. Ovcharenko, F. D.; Ulberg, Z. R.; Petrov, N. V. V. I. Mendeleev All-Union Chem Soc J 1989, 34, 159.
36. Mitskevich, T. N. Russ J Coord Chem 1986, 12, 418.
37. Kukushkin, Y. N. Russ J Coord Chem 1983, 12, 147.
38. Tager, A. A. Physical Chemistry of Polymers (in Russian); Khimia: Moscow, 1984.
39. Frolov, Y. R.; Gradsky, A. S. V. I. Mendeleev All-Union Chem Soc J 1989, 34, 182.
40. Ovcharenko, F. D.; Morau, V. N.; Moran, L. E. Russ Colloid J 1980, 42, 880.
41. Bryk, M. T.; Danilenko, E. E. Ukr Chem J 1988, 54, 355.
42. Shunsuke, S.; Yoshio, M. J Chem Soc Jpn Ind Chem 1973, 185.
43. Furman, A. A. Inorganic Chlorides (in Russian); Khimia: Moscow, 1980.
44. Lukachina, V. V. Ligand–Ligand Interactions and Stability of Complexes Containing Different Ligands (in Russian); Naukova Dumka: Kiev, 1988.